

Microlens Formation in Microgel/Gold Colloid Composite Materials via Photothermal Patterning

Clinton D. Jones, Michael J. Serpe, Laura Schroeder, and L. Andrew Lyon*

School of Chemistry and Biochemistry, Georgia Institute of Technology, Atlanta, Georgia 30332-0400

Received January 8, 2003; E-mail: lyon@chemistry.gatech.edu

Three-dimensional (3D) microstructures have gained interest over the years due to the potential use in electric, photonic, and biochemical fields. The formation of microstructures is commonly achieved through direct laser writing¹ and photolithography.² Also of current interest is the assembly of colloidal particles to create patterned microstructures. Several methods have been developed to achieve this type of assembly and include using patterned self-assembled monolayer films,³ electrodes,⁴ and micromolds.⁵ We report here on the formation of a microlens inside of hydrogel colloidal crystal assemblies by a newly developed photothermal approach.

In this patterning method, ~226-nm diameter colloidal hydrogel particles composed of the thermoresponsive polymer poly(*N*-isopropylacrylamide) (pNIPAm) are coassembled with 16 ± 1.6 nm colloidal Au. This affords composite materials that can be locally interconverted between a glassy, disordered state and a crystalline, ordered state when addressed with light at a wavelength ($\lambda = 532$ nm) nearly resonant with the Au nanoparticle plasmon absorption at ~520 nm.⁶ The Au acts as a localized heat source due to the large extinction coefficient of Au nanoparticles at the plasmon resonance ($\sim 1 \times 10^9$ M⁻¹ cm⁻¹ at 520 nm for 20-nm diameter colloidal Au) and the small photoemission quantum yield for such particles.⁷ The energy absorbed upon plasmon excitation is re-emitted via nonradiative pathways, thereby heating the local surroundings inside the sample. Cycling the temperature across the volume phase transition temperature (VPTT) of the microgels (~32 °C) produces an entropically favored phase separation event in which the vast majority of the water is expelled from the network.⁸ This transition manifests itself as a large particle size change. The hydrogel particles are then able to diffuse more readily than in their swollen state, thus allowing for crystal nucleation and growth within the laser spot. These irradiation conditions are apparently ideal to produce a local temperature increase that is appropriate for annealing the assembly to the crystalline state from the glassy state.

Microgels were prepared via aqueous free-radical precipitation polymerization, purified, and characterized by dynamic light scattering as previously reported.⁹ Colloidal Au was prepared via citrate reduction of HAuCl₄ according to methods previously reported.¹⁰ To form composite colloidal crystals, a solution containing 1.25 mL of purified microgel solution and 0.25 mL of the colloidal Au solution was placed into a centrifuge tube and centrifuged at 26 °C, at a relative centrifugal force of 16 100g for 75 min; the clear, colorless supernatant solution was removed following centrifugation. Colloidal Au was redispersed throughout the microgel pellet by repeated heating (35 °C), agitating, and sonicating. The sample was then heated to 35 °C and injected into a cell with a total volume of 0.057 mL consisting of an oval 19 × 6 × 0.5 mm perfusion gasket (Molecular Probes) sandwiched between two microscope cover glasses (22 × 22 mm, Fisher). Fast cooling of the sample yielded the kinetically trapped bulk glassy state of the colloidal crystals.

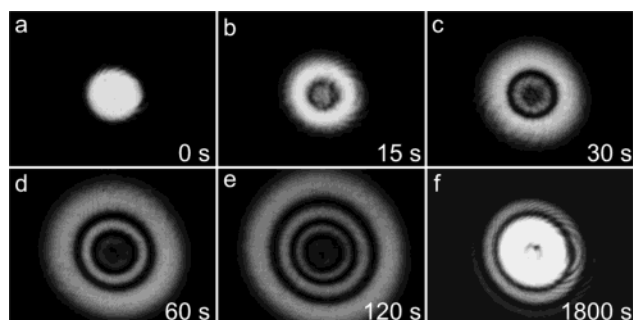
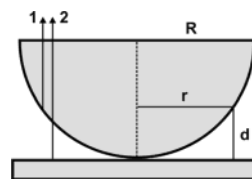


Figure 1. A series of black and white CCD images of transmitted laser light showing the evolution of interference rings over time. The composite material was placed 5 cm above the vertically positioned laser source, and the CCD camera was positioned 14 cm on the opposite side of the sample to collect transmitted light. (a) 0, (b) 15, (c) 30, (d) 60, (e) 120, (f) 1800 s.

Scheme 1. Representation of a Plano-convex Lens Resting on a Planar Surface



A 532 nm pulsed Nd:YAG (Uniphase) was used as a laser source. The temperature of the sample was controlled during irradiation with a Physitemp TS-4 programmable temperature stage. Photothermal crystallization was performed by placing the sample cell on the temperature stage located 5 cm (incident laser power of 0.87 W/cm²) above the vertically positioned Nd:YAG laser source. Irradiation for 40 min at 21 °C produced a crystallized region in the area of the beam. Laser light that is transmitted through a sample during irradiation produces a collection of concentric rings as shown in Figure 1. The formation of interference rings was monitored with a Javelin (JE-7442) b/w CCD camera placed 14 cm from the sample on the opposite side of laser irradiation. The number, spacing, and diameter of these rings increase over time, reaching steady state after ~1200 s. When the sample is irradiated horizontally, as opposed to the vertical conditions shown here, the rings do not evolve into a symmetric pattern. Asymmetry is thought to be the result of gravitational effects, as the irradiated region begins to flow slightly due to a decrease in sample viscosity as the temperature in the focal volume increases.

As stated above, ring formation is a temporally and spatially dynamic process. Diffraction resulting from crystal planes would not explain this behavior, assuming a constant lattice spacing is present as the crystalline region is formed. The evolving ring pattern can be explained by considering the phenomenon of Newton's rings.¹¹ Scheme 1 illustrates the ideal case for a glass plano-convex lens with a radius of curvature R resting on a planar glass surface

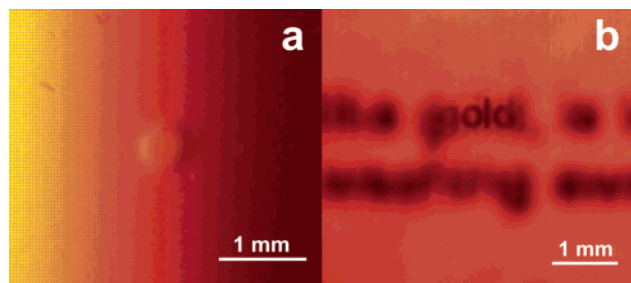


Figure 2. (a) A photographic image of an irradiated sample showing that the patterned region has a three-dimensional structure and is hemispherical in shape. A backlight was used to adjust the contrast of the structure, which appears red due to the presence of colloidal Au. (b) Two lines of text as seen through a microlens illustrating the focusing ability. The lens is located over the word “gold”, which is the only word within the two lines that is legible. The text on white paper is located 1.7 cm behind the sample.

in air. The formation of a ring pattern occurs when monochromatic light interferes with the varying thickness of air between the lens and the planar surface. Reflection of monochromatic light may occur at the underside of the lens (ray 1) or at the top of the planar surface (ray 2) because of the differences in refractive indices of the media. Ray 1 does not undergo a phase change upon reflection at the air interface, while ray 2 undergoes a phase change of π upon reflecting off the optically denser medium. Thus, the total apparent path difference between the two rays is a combination of a phase change of $\lambda/2$ and the physical distance of d . Along the curved surface of the lens at a distance r from the point of contact, reflection may occur at a point d from the planar surface, and interference will occur. One may deduce the following relationship

$$r_n^2 = (2R - d)d \quad (1)$$

where r_n represents the n th order point along the curved surface. The radius and the number of interference rings will change with the radius of curvature and thus the distance d from the planar surface. Similar behavior is shown in Figure 1, where the number, spacing, and diameter of the interference rings change over time as the lens is formed.

A photographic image of a microlens is shown in Figure 2a and illustrates the three-dimensional structure of the irradiated region. This photograph was taken of the sample on the opposite side from which laser irradiation was performed. The structure appears curved and seems to project out toward the viewer from the plane of the image. We hypothesize that the Gaussian beam profile of the incident laser light contributes to this shape. Assuming a homogeneous distribution of Au colloid within the region being irradiated, we found that the temperature in the middle of the illuminated region is likely highest due to a greater flux of photons. Apparently, the temperature near the periphery of the circular region is lower than the central portion and produces conditions ideal for local crystallization at the periphery of the laser spot, serving as a template for crystal growth (Supporting Information). Figure 2b shows the focusing ability of the microlens. In this case, the illuminated side of the sample is closest to the photographic source. Two lines of black text on white paper were placed behind the

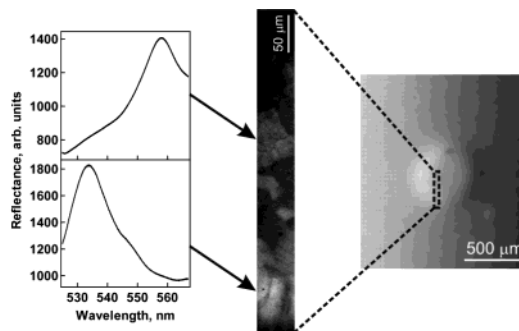


Figure 3. Microspectrophotometric analysis of the microlens shows a redshift in the Bragg peak from the periphery toward the inside. This change in lattice constant indicates that the refractive index changes radially within the irradiated region (Supporting Information).

sample, and the irradiated region was positioned over the word “gold” in the top line. The position of the text was varied behind the sample until focusing was achieved.

Equation 1 requires only a difference in the refractive indices of the involved media. Figure 3 shows the shift in Bragg reflectance within the microlens region. A larger lattice constant near the center of the lens indicates that individual microgels are more hydrated than those near the periphery. Differing degrees of particle hydration provide the refractive index difference required for a working lens. The overall refractive index of the crystalline region is also apparently different from that of the surrounding overpacked glassy region, thus allowing lensing to occur.

In summary, we show the ability of a photothermally patterned area inside of microgel/Au nanoparticle composite materials to act as a microlens. This lensing is possible due to a radially varying refractive index in the lens. This is observable as radial distribution of crystal lattice constants, which arises from the use of a Gaussian “writing” beam. Microlens formation is a dynamic process and can be temporally monitored and modeled by a phenomenon similar to that which causes Newton’s rings.

Acknowledgment. L.A.L. thanks the Arnold and Mabel Beckman Foundation for a Young Investigator Award. We also thank Prof. Robert Dickson for the use of the Nd:YAG laser.

Supporting Information Available: Bright-field reflectance image of the lens and associated microspectrophotometric data (PDF). This material is available free of charge via the Internet at <http://pubs.acs.org>.

References

- (1) Gale, M. T.; Rossi, M.; Pedersen, J.; Schutz, H. *Opt. Eng.* **1994**, *33*, 3556–3566.
- (2) Wu, H. K.; Odom, T. W.; Whitesides, G. M. *Anal. Chem.* **2002**, *74*, 3267–3273.
- (3) Tien, J.; Terfort, A.; Whitesides, G. M. *Langmuir* **1997**, *13*, 5349–5355.
- (4) Hayward, R. C.; Saville, D. A.; Aksay, I. A. *Nature* **2000**, *404*, 56–59.
- (5) Kim, E.; Xia, Y. N.; Whitesides, G. M. *Adv. Mater.* **1996**, *8*, 245.
- (6) Jones, C. D.; Lyon, L. A. *J. Am. Chem. Soc.* **2003**, *125*, 460–465.
- (7) Link, S.; El-Sayed, M. A. *Int. Rev. Phys. Chem.* **2000**, *19*, 409–453.
- (8) Pelton, R. *Adv. Colloid Interface Sci.* **2000**, *85*, 1–33.
- (9) Jones, C. D.; Lyon, L. A. *Macromolecules* **2000**, *33*, 8301–8306.
- (10) Grabar, K. C.; Freeman, R. G.; Hommer, M. B.; Natan, M. J. *Anal. Chem.* **1995**, *67*, 735–743.
- (11) Jenkins, F. A. *Fundamentals of Optics*, 2nd ed.; McGraw-Hill: New York, 1950.

JA034076H